

See discussions, stats, and author profiles for this publication at: <https://www.researchgate.net/publication/50940678>

# Energy transfer cassettes in silica nanoparticles target intracellular organelles

ARTICLE *in* ORGANIC & BIOMOLECULAR CHEMISTRY · MARCH 2011

Impact Factor: 3.56 · DOI: 10.1039/c0ob00967a · Source: PubMed

---

CITATIONS

3

READS

22

## 9 AUTHORS, INCLUDING:



Jiney Jose

University of Auckland

20 PUBLICATIONS 286 CITATIONS

[SEE PROFILE](#)



Aurore Loudet

Texas A&M University

19 PUBLICATIONS 2,188 CITATIONS

[SEE PROFILE](#)



Rola Barhoumi

Texas A&M University

125 PUBLICATIONS 2,765 CITATIONS

[SEE PROFILE](#)



Robert C Burghardt

Texas A&M University

268 PUBLICATIONS 9,524 CITATIONS

[SEE PROFILE](#)

Cite this: *Org. Biomol. Chem.*, 2011, **9**, 3871

[www.rsc.org/obc](http://www.rsc.org/obc)

PAPER

## Energy transfer cassettes in silica nanoparticles target intracellular organelles†

Jiney Jose,<sup>a</sup> Aurore Loudet,<sup>a</sup> Yuichiro Ueno,<sup>a</sup> Liangxing Wu,<sup>a</sup> Hsiang-Yun Chen,<sup>a</sup> Dong Hee Son,<sup>a</sup> Rola Barhoumi,<sup>b</sup> Robert Burghardt<sup>b</sup> and Kevin Burgess<sup>\*a</sup>

Received 1st November 2010, Accepted 3rd March 2011

DOI: 10.1039/c0ob00967a

Lipophilic energy transfer cassettes like **1** and **2** are more conveniently synthesized than the corresponding hydrophilic compounds, but they are not easily used in aqueous media. To overcome the latter issue, cassettes **1** and **2** were separately encapsulated in silica nanoparticles (*ca.* 22 nm) which freely disperse in aqueous media. Photophysical properties of the encapsulated dyes **1–SiO<sub>2</sub>** and **2–SiO<sub>2</sub>** were recorded. The nanoparticles **1–SiO<sub>2</sub>** permeated into Clone 9 rat liver cells and targeted only the ER. A high degree of energy transfer was observed in this organelle such that most of the light fluoresced from the acceptor part, *i.e.* the particles appeared red. Silica nanoparticles **2–SiO<sub>2</sub>** also permeated into Clone 9 rat liver cells and they targeted mitochondria but were also observed in endocytic vesicles (lysosomes or endosomes). In these organelles they fluoresced red and red/green respectively. Thus the cargo inside the nanoparticles influences where they localize in cells, and the environment of the nanoparticles in the cells changes the fluorescent properties of the encapsulated dyes. Neither of these findings were anticipated given that silica nanoparticles of this type are generally considered to be non-porous.

### Introduction

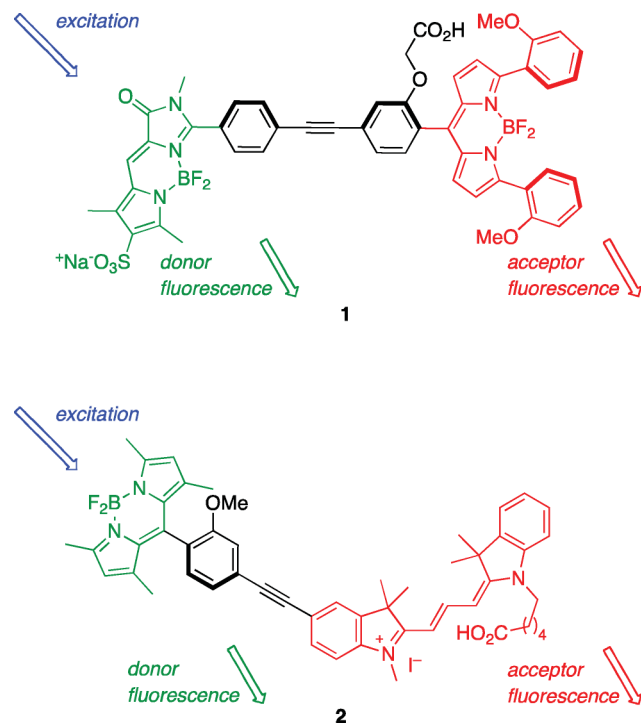
Fluorescent dyes functionalized with –Si(OR)<sub>3</sub> groups can be used as nuclei about which non-porous silica nanoparticles (radii as small as 10–15 nm)<sup>1,2</sup> can be formed. These silica nanoparticles disperse freely in aqueous media where they can be stored without aggregation for several months. Consequently, SiO<sub>2</sub>-encapsulation can be used to bring poorly water soluble fluorescent dye cargoes into aqueous environments.

Our group is interested in the design, synthesis, and applications of energy transfer cassettes like **1** and **2**.<sup>3–6</sup> Basically, these have donor parts that absorb light relatively strongly in a convenient region (*e.g.* 488 nm). Energy from this excitation that emerges as fluorescence from the donor part appears green (*e.g.* 530 nm). However, if there is rapid energy transfer to the acceptor parts then the cassette will fluoresce red (*e.g.* 600 nm). Ratios of donor emission-to-acceptor emission (or “green-to-red”) fluorescence from these cassettes can be informative. For instance, in previous work we identified a cassette that sensed protons in the medium, hence green-to-red fluorescence ratios could be used in measurements of intracellular pH.<sup>7,8</sup>

<sup>a</sup>Department of Chemistry, Texas A&M University, Box 30012, College Station, TX 77842, USA. E-mail: burgess@tamu.edu

<sup>b</sup>Department of Veterinary Integrative Biosciences, Texas A&M University, College Station, TX 77843, USA. E-mail: rburghardt@cvm.tamu.edu

† Electronic supplementary information (ESI) available: Synthesis and characterization information for silica nanoparticles and cellular imaging studies. See DOI: 10.1039/c0ob00967a



Syntheses of lipophilic cassettes like **1** and **2** are non-trivial, involving multiple steps. It is significantly harder to make analogs of these systems functionalized with water-solubilizing groups. This is unfortunate because energy transfer cassettes tend to be

more useful in biotechnology if they are compatible with aqueous media. Approaches to circumvent these problems are therefore valuable.

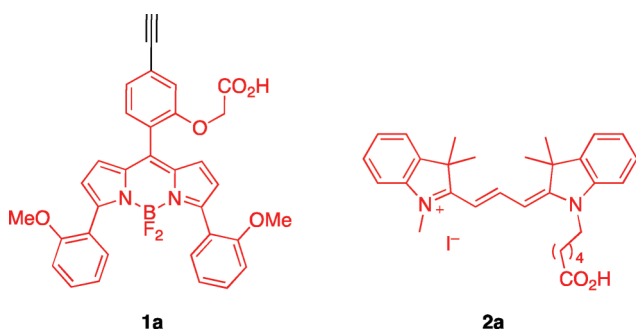
This paper reports on silica nanoparticles formed about the lipophilic cassettes **1** and **2**. This study was initiated as a strategy to bring the cassettes into aqueous media. However, since this is the first report of energy transfer cassettes in silica nanoparticles, we were also curious to investigate the photophysical properties of the encapsulated dyes, and the behaviour of the particles in cells.

In fact, there have been few reports of import and localization of *any* dye-labeled non-porous silica nanoparticles in cells<sup>9–12</sup> (though larger *porous* silica nanoparticles have been investigated more extensively<sup>12–22</sup>). In one, 15 nm particles loaded with a 3,5-difuranylvinyl-BODIPY dye, (but without special surface functional groups) have been observed to accumulate in the cytoplasm of Cos-1 cells.<sup>23</sup> In another, 20 nm silica nanoparticles were doped with rhodamine-B and surface was functionalized with various bioactive molecules such as transferrin, or monoclonal antibodies like anti-claudin 4 and anti-mesothelin for targeted delivery to pancreatic cancer cells.<sup>24</sup> In summary, the focus of the literature in this area has been on targeting,<sup>25–27</sup> transfection,<sup>26,28,29</sup> photodynamic therapy,<sup>30–32</sup> or drug delivery, but the fate of the nanoparticles inside cells has received little attention.

## Results and discussion

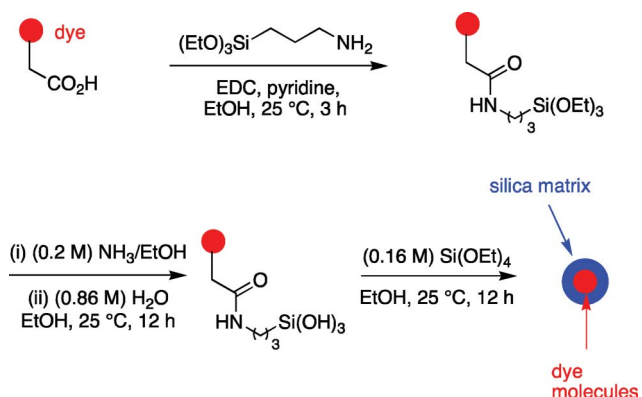
### Encapsulation of cassettes **1–2** in silica nanoparticles

Syntheses of the cassettes **1** and **2** will be published elsewhere. Cassette **1** in pH 7.4 phosphate buffer has poor solubility, even for fluorescence experiments, and it dissolves extremely slowly. Probe **2** was observed to be even less soluble in aqueous media.



Encapsulation of the cassettes and of the corresponding acceptors **1a–2a** (controls) was achieved *via* slight modifications (reaction times; see ESI†) of a literature procedure.<sup>33</sup> Thus the cassettes were conjugated *via* their activated carboxylic acid groups to 3-aminopropyltriethoxysilane (APTS; Scheme 1). The silica nanoparticles were obtained in pH 7.4 sodium phosphate buffer (0.1 M) *via* a series of dialysis steps (the particles could not, in our hands, be dried from one solvent then resuspended in another). Consequently, it was possible to study the encapsulated cassettes in aqueous media whereas the parent systems are insufficiently soluble to do this.

TEM images of the nanoparticles (Fig. 1) showed they were spherical, well dispersed, and homogeneous in size, with an average diameter of 20–24 nm. No degradation was observed when they were continuously subjected to the TEM electron beam for *ca.* 30 min, indicating the particles were physically robust.



**Scheme 1** Syntheses of dye-doped silica nanoparticles.

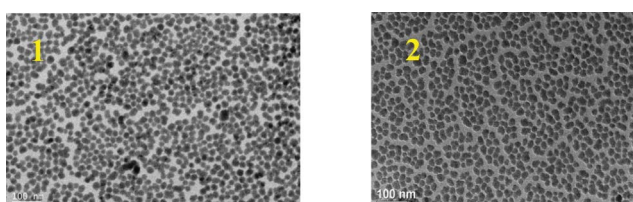


**Fig. 1** TEM images of silica nanoparticles doped with cassettes **1** and **2** (left and right); particle size: 20–24 nm.

Particle sizes for the acceptors **1a** and **2a** encapsulated in silica nanoparticles were in the similar range (see ESI Figure S1†).

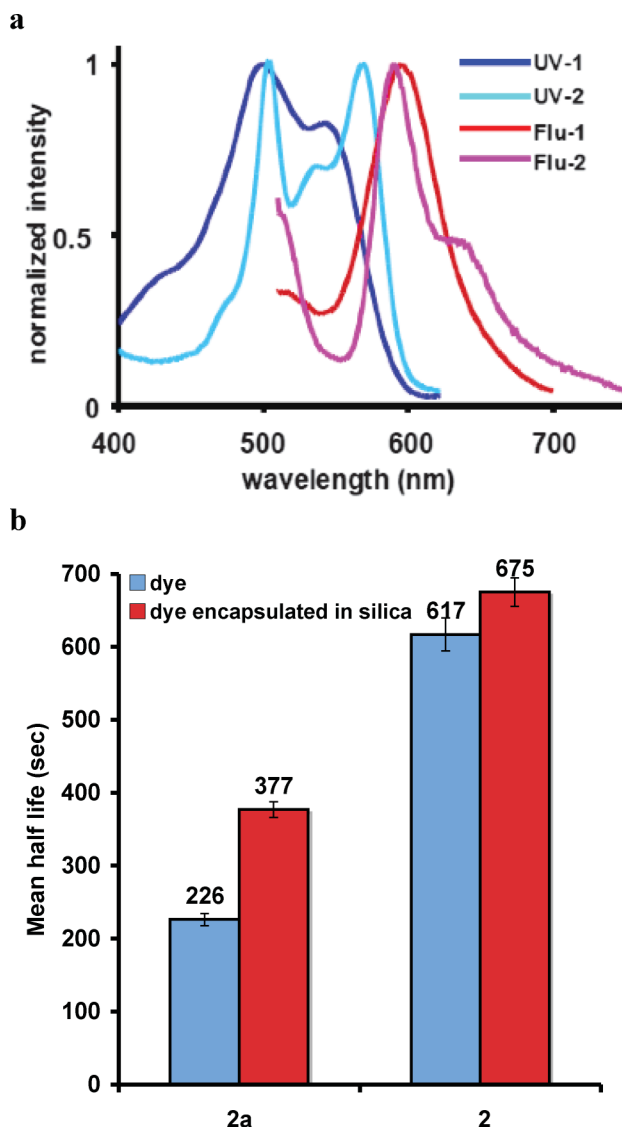
### Photophysical properties of silica nanoparticles in aqueous media

Fig. 2a shows the absorbance and emission maxima of cassettes **1** and **2** encapsulated in silica nanoparticles dispersed in pH 7.4 phosphate buffer. The cassettes each have two distinct absorbance maxima corresponding to their donor and acceptor fragments. We have defined the ratio of the fluorescence quantum yields of cassettes when excited at the donor to that when excited at the acceptor as the *energy transfer efficiency* (ETE).<sup>6</sup> This parameter for the encapsulated cassettes is high: 93 and 78%, for **1–SiO<sub>2</sub>** and **2–SiO<sub>2</sub>**, respectively (Table 1). The overall quantum yield for **2–SiO<sub>2</sub>** is significantly lower than for cassette **1–SiO<sub>2</sub>**. The free dyes **1** and **2** are not soluble enough in aqueous media for photophysical

**Table 1** Photophysical properties in pH 7.4 (0.1 M sodium phosphate buffer)

	Free dyes (EtOH)		Silica nanoparticles (pH 7.4)	
	<b>1</b>	<b>2</b>	<b>1–SiO<sub>2</sub></b>	<b>2–SiO<sub>2</sub></b>
$\lambda_{\text{max ab}}$ (nm)	498, 543	504, 569	499, 544	504, 568
$\lambda_{\text{max emiss}}$ (nm)	600	590	597	592
$\Phi_D^a$	0.46+/−0.02 <sup>c</sup>	0.20+/−0.01 <sup>c</sup>	0.31 ± 0.02 <sup>c</sup>	0.04 <sup>d</sup>
$\Phi_A^b$	0.48+/−0.01 <sup>c</sup>	0.22+/−0.02 <sup>d</sup>	0.33 ± 0.01 <sup>c</sup>	0.05 <sup>d</sup>
ETE %	96	90	93	78

<sup>a</sup>  $\Phi_D$ : quantum yield of cassette when excited at the donor absorption maxima; <sup>b</sup>  $\Phi_A$ : quantum yield of cassette when excited at the acceptor absorption maxima; standards used for quantum yield measurement were: <sup>c</sup> rhodamine 6G ( $\Phi$  0.92 in EtOH);<sup>37</sup> <sup>d</sup> rhodamine 101 ( $\Phi$  1.0 in EtOH).<sup>38</sup> Quantum yields were measured three times and averaged.



**Fig. 2** **a** UV absorbance and fluorescence of cassettes **1** and **2** encapsulated in silica in 0.1 M phosphate buffer pH 7.4 (*ca.*  $10^{-6}$  M for UV and  $10^{-7}$  M for fluorescence). Cassettes are excited at the corresponding donor absorption maxima. **b** Photobleaching half-lives for the acceptor **2a** and cassette **2** without (blue) and with (red) silica encapsulation. The error bars represent two values of mean half-life measured. The average value is shown for **2** and **2a**.

measurements, but data for them in EtOH are included in Table 1 as a closest possible comparison.

Acceptor **1a** encapsulated in silica had low quantum yield in EtOH and pH 7.4 compared to free acceptor. For acceptor **2a** (Cy3) encapsulated in silica, the quantum yield was slightly higher in EtOH and almost 9 fold higher in pH 7.4 compared to free acceptor (ESI,† Tables S1 and S2).

Quantum yields of fluorescent dyes tend to be enhanced by encapsulation in non-porous silica nanoparticles, but here encapsulation had little effect for cassette **1** and the quantum yield of **2** decreased.<sup>2</sup> The data collected here do not enable us to determine why the quantum yield of **2-SiO<sub>2</sub>** is relatively low in silica, but it could be due to an aggregation effect of the dyes in the particles.<sup>34,35</sup>

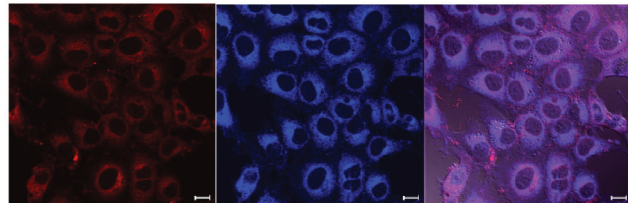
Tight encapsulation of dyes in non-porous silica matrices may diminish their rates of reaction with oxygen, and decrease their rate of photobleaching.<sup>34,36</sup> Photobleaching rates were measured for **2-SiO<sub>2</sub>** and the corresponding acceptor **2a** (Fig. 2b). Encapsulation of the cyanine-acceptor **2a** made this fluor significantly more photostable. The photostability of cassette **2** was also increased upon encapsulation, but to a lesser extent. These data are consistent with the notion that photobleaching is often a result of interaction between the fluorophore and dissolved oxygen in solvent. The silica matrix seems to protect the encapsulated fluorophore from interactions with dissolved oxygen, and this gives the nanoparticles more stability to photobleaching.

### Import of cassettes **1-2** encapsulated in silica nanoparticles into cells

Uptake of the cassettes encapsulated in silica nanoparticles into Clone 9 rat liver cells was investigated to test for cytotoxicity, cell permeability, and organelle targeting. Silica nanoparticles have been shown to be non-cytotoxic at concentrations up to  $0.1\text{ mg mL}^{-1}$ .<sup>39</sup> Consistent with this, no significant cytotoxic effects were observed when the cells were treated with the nanoparticles prepared in this work.

Efficient uptake of the particles was observed after 2 h at 37 °C. The **1-SiO<sub>2</sub>** nanoparticles specifically targeted *only* the ER (Fig. 3a). Energy transfer for **1-SiO<sub>2</sub>** in this organelle was complete within the limits of the observation (Fig. 3b).

**a** *1-SiO<sub>2</sub>* colocalizes with ER Tracker Blue-White



**b** *1-SiO<sub>2</sub>* accumulates only in the ER, and perfect energy transfer is observed

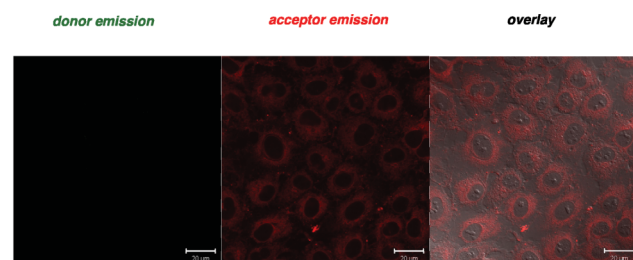
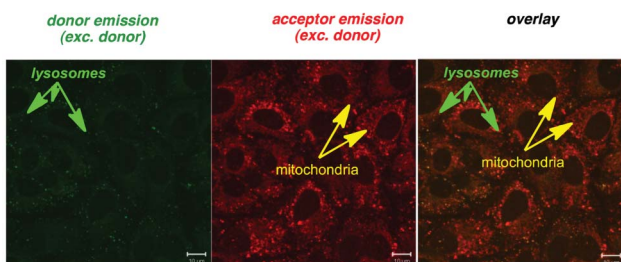


**Fig. 3** Fluorescence of: **a** cassette **1-SiO<sub>2</sub>** and ER-Tracker™ Blue-White DPX; and, **b** cassette **1-SiO<sub>2</sub>** in Clone 9 cells. Part **a** shows that the nanoparticles **1-SiO<sub>2</sub>** *only* accumulate in the ER, and perfect energy transfer is observed. Throughout the cassette was excited at 488 nm *i.e.* at the donor part. Donor and acceptor emission were observed using Band Pass (BP) 500–530 and BP 565–615 emission filters, respectively. Fluorescence images from ER-Tracker™ Blue-White DPX were collected using the following filter set: excitation at 740 nm, emission BP 435–485, respectively. Scale bar (a) 10 μm (b) 20 μm.

**a 2-SiO<sub>2</sub>** emits green/red in the lysosomes and/or endosomes, and only red in the mitochondria when excited at the donor



**b 2-SiO<sub>2</sub>** emits red only in the mitochondria and lysosomes and/or endosomes when excited at the acceptor

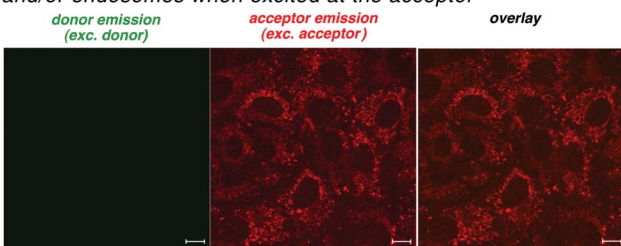


**Fig. 4** Fluorescence of cassette **2-SiO<sub>2</sub>** when excited at the: **a** donor part i.e. 488 nm; and, **b** acceptor part i.e. 543 nm in Clone 9 cells. Part **a** shows accumulation of the nanoparticles **2-SiO<sub>2</sub>** in the endocytic vesicles (lysosomes and/or endosomes) (green/red), and mitochondria (red). Part **b** shows the nanoparticles accumulate in the mitochondria and the lysosomes and/or endosomes. Fluorescence images from the donor and acceptor emission were observed using the following filter set: excitation at 488 nm or 543 nm, for excitation at the donor and acceptor, respectively, emission BP 500–530 and BP 565–615 for the donor and acceptor, respectively. Scale bar 10 μm.

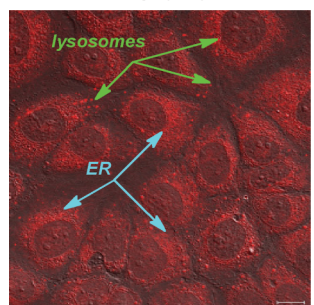
Import of **2-SiO<sub>2</sub>** resulted in labeling of the mitochondria and endocytic vesicles (lysosomes and/or endosomes) (Fig. 4). Perfect energy transfer (only red emission), was observed in the mitochondria. However, in the vesicles, fluorescence was now observed in both the red and green channels, indicating *partial energy transfer*.

A summary of the data from these studies is as follows. The **1-SiO<sub>2</sub>** particles were *selective* for targeting the ER and showed near perfect energy transfer. The **2-SiO<sub>2</sub>** system was selective for the mitochondria wherein it showed perfect energy transfer and also for lysosome, wherein partial energy transfer (both green and red emissions) was observed.

For completeness, silica nanoparticles containing the acceptor fragments **1a** and **2a**, were also prepared and tested. Uptake of **1a-SiO<sub>2</sub>** gave (after 2 h) labeling of the ER and lysosomes, while under similar conditions (3 h) **2a-SiO<sub>2</sub>** targeted the mitochondria (Fig. 5). These data contrast with those obtained for the corresponding cassettes (above) where **1-SiO<sub>2</sub>** were *more* organelle selective (targeted only the ER). These observations indicate the targeting effect is not solely based on the acceptor fragment.

To confirm the uptake of the silica nanoparticles, TEM was performed on one illustrative system: Clone 9 cells were treated with **1a-SiO<sub>2</sub>**. This analysis showed internalization of the nanoparticles into intracytoplasmic vacuoles or endosomes. Free nanoparticles were also observed in the cytoplasm, suggesting that they are able to escape from the endosomes and resist degradation. In fact, we

**a 1a-SiO<sub>2</sub>**  
combined fluorescence images  
with Differential Interference Contrast  
image (DIC)



**b 2a-SiO<sub>2</sub>**  
combined fluorescence images  
with Differential Interference Contrast  
image (DIC)

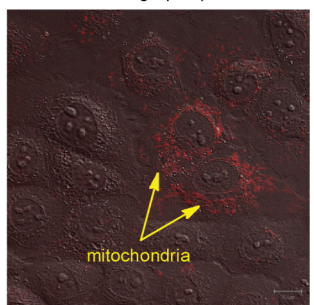


**Fig. 5** Intracellular fluorescence of *SiO<sub>2</sub>*-nanoparticles from **a** acceptor **1a**; and, **b** acceptor **2a**. Combined fluorescence images with differential interference contrast image (DIC). Fluorescence images from the acceptor emission were observed using the filter BP 565–615 for excitation at 543 nm. Scale bar 10 μm.

were able to observe by TEM the rupture of an endosome and liberation of the nanoparticles in the cytoplasm (Fig. 6).

## Conclusions

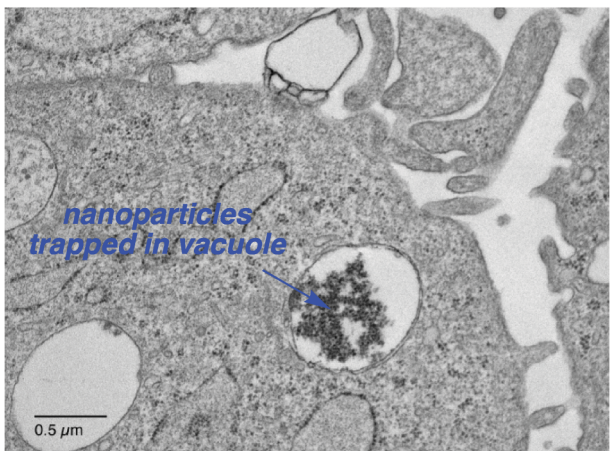
Fig. 7 summarizes the data obtained by importing *silica-encapsulated* system **1-SiO<sub>2</sub>** and **2-SiO<sub>2</sub>** into cells. There are two surprising, and possibly related, aspects of these observations. First, *the cargoes impact the regions in the cell where the nanoparticles accumulate*. Second, *the energy transfer efficiencies of the cargoes in the nanoparticles (hence the color of the fluorescence emissions) can be impacted by the nanoparticle's cellular environment*. Taken together, this leads us to conclude that the cargoes are somewhat exposed to the surface environment of the nanoparticles.

Selective targeting of nanoparticles inside cells might be anticipated based on size considerations; relatively large entities might be inclined to become stuck in some parts of the cell. However, this work shows that particles from **1** target the ER whereas those from **2** accumulate in different places: the mitochondria and lysosomes. Thus the attraction of the non-porous nanoparticles for certain organelles is not purely physical.

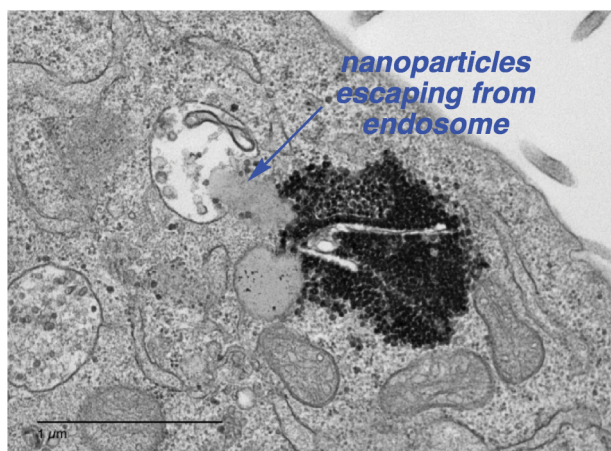
Encapsulation in non-porous silica is generally considered to shield dye cargoes from the solvent environment, and tends to increase their quantum yields.<sup>2</sup> However, only a fraction of the total cargo would need to protrude from the nanoparticle surface to give an organelle-targeting effect. Furthermore, fluorescence from combinations of fluor fragments in energy transfer cassettes is a more complicated phenomenon than for single fluors, hence correlations between encapsulation and enhanced fluorescence are likely to be less straightforward. This accounts for the different affects encapsulation had on the cassettes.

A corollary to the conclusions presented above relates to the fraction of cargo exposed to the surface. There must be enough to change the color of the fluorescence from the nanoparticles *as a whole* when they are impacted by different cellular environments. Perhaps significantly, variation of the fluorescence was observed only for **2-SiO<sub>2</sub>**, for which the percentage energy transfer in the nanoparticles in solution was only 78%. The color did not appear

a  $1a\text{-SiO}_2$  is internalized in intracytoplasmic vacuoles or endosomes



b  $1a\text{-SiO}_2$  can escape from endosomes



c  $1a\text{-SiO}_2$  resists endosomal degradation and is free in the cytoplasm

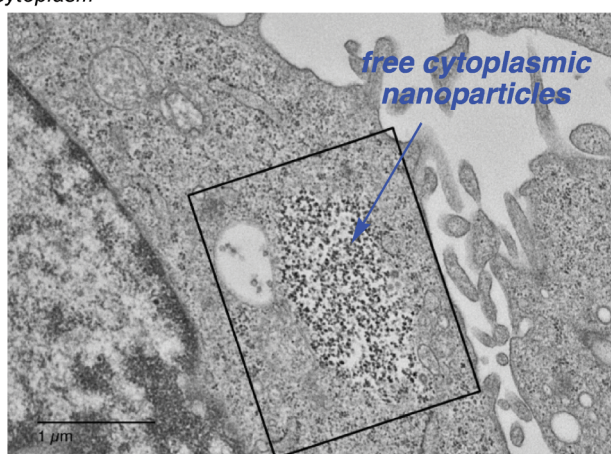


**Fig. 6** TEM images of Clone 9 cells treated with  $\text{SiO}_2$ -nanoparticles from acceptor **1a**. Part a shows that the  $\text{SiO}_2$ -nanoparticles are internalized in intracytoplasmic vacuoles or endosomes. In part b, these nanoparticles are seen escaping the endosome. Part c shows free cytoplasmic nanoparticles, indicating the nanoparticles can resist endosomal degradation.

to change with cellular environment for **1-SiO<sub>2</sub>**, for which near complete energy transfer was observed for the particles in

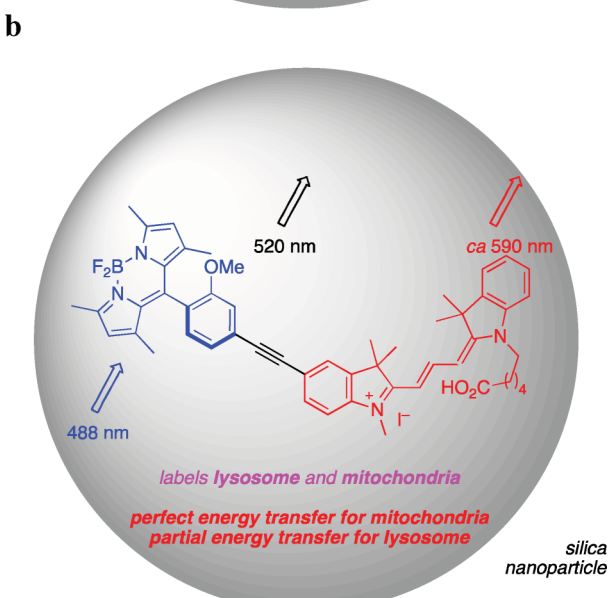
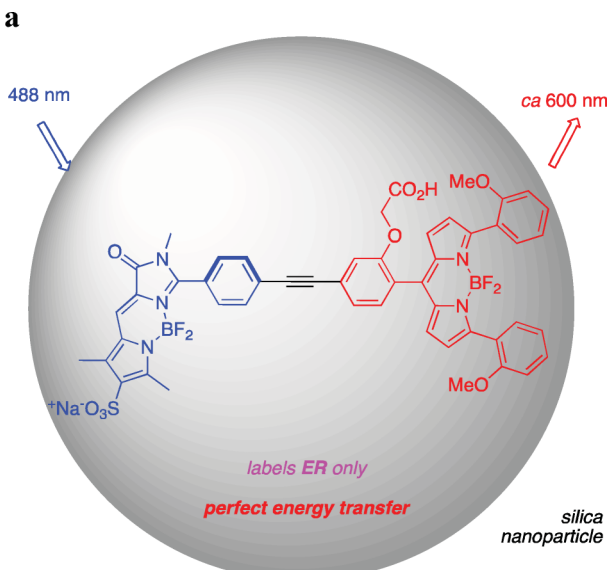


**Fig. 7** Summary of data from cell localization of the cassette encapsulated silica nanoparticles **a**  $1\text{-SiO}_2$ ; and, **b**  $2\text{-SiO}_2$ .

water. It follows that this difference might simply imply that cassette **2** is more environment sensitive than **1**, possibly because the cyanine acceptor of **2** is charged whereas the acceptor in **1** is a neutral BODIPY dye. Indeed, cyanine dyes in cells are known to be sensitive to membrane potentials and other effects related to their immediate environment.<sup>40,41</sup>

For amorphous silica nanoparticles it is not easy to differentiate between ones with the cargo neatly contained in an inner sphere or “sea-mane-like” structures with some of the cargo making small protrusions from the surface (Fig. 8). Moreover, the degree of protrusion of the cargo from within a nanoparticle may vary with the structure of the cargo. This notion is important for interpretation of the data presented in this paper.

We find the discovery that through-bond energy transfer can be organelle specific interesting. It implies that dyes encapsulated in silica nanoparticles might be deliberately designed to exploit this

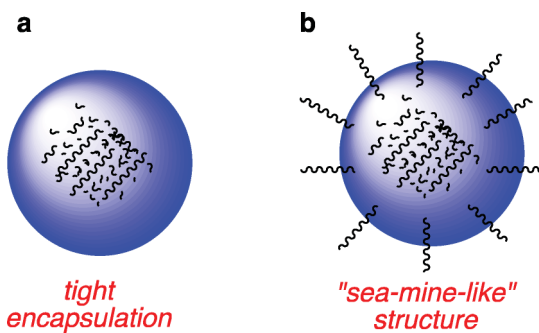


**Fig. 8** Fluor cargoes in amorphous nanoparticles can be: **a** tightly packed at the core; or, **b** randomly dispersed with some surface exposed dye molecules.

phenomenon. Particles that change color in different organelles provide a new dimension to probes for intracellular imaging.

## Experimental

See the ESI† for detailed synthesis and characterization information for silica nanoparticles and cellular imaging studies.

### General procedure for synthesis of silica nanoparticles

The encapsulation of cassettes and corresponding acceptors was achieved by following a reported procedure by Wiesner *et al.* with slight modification.<sup>33</sup> The organic dye is conjugated *via* activated carboxylic acid group to 3-aminopropyltriethoxysilane (APTS) at a molar ratio of 1:50 (fluorophore:APTS) in degassed absolute EtOH (1.0 mL, 200 proof) under nitrogen. The above dye solution (0.14 mL,  $1.7 \times 10^{-5}$  M) was added to EtOH (200% proof) along with deionized water (1.52 mL, 0.86 M) and NH<sub>3</sub> in EtOH (5.0 mL, 0.2 M) at 25 °C to make up a final volume of 50 mL and stirred for 12 h at 25 °C. TEOS (1.63 mL, 0.16 M) was then added in aliquots of 0.4 mL every fifteen minutes and stirring continued for another 12 h at 25 °C. The resulting silica nanoparticles were dialyzed into EtOH to removed unreacted starting materials using a Spectra/Por dialysis membrane with molecular weight cut off (MWCO) 6000–8000 for 12 h. Further dialysis was performed to transfer the formed silica nanoparticles from EtOH to deionized water and finally to pH 7.4 (0.1 M sodium phosphate buffer).

### Cell culture

Clone 9 normal rat liver cells (American Type Culture Collection) were cultured as subconfluent monolayers on 75 cm<sup>2</sup> culture flask with vent caps in Ham's medium supplemented with 10% fetal bovine serum (FBS) in a humidified incubator at 37 °C with 5% CO<sub>2</sub>. Cells grown to subconfluence were enzymatically dissociated from the surface with trypsin and plated 2–3 days prior to the experiments in Lab-Tek two well chambered coverglass slides (Nunc).

### Fluorescence microscopy

Uptake and subcellular localization of the cassette doped silica nanoparticles **1–SiO<sub>2</sub>**, **2–SiO<sub>2</sub>**, **1a–SiO<sub>2</sub>**, and **2a–SiO<sub>2</sub>** were studied on living Clone 9 normal rat liver cells using a Zeiss 510 META NLO Multiphoton Microscope System consisting of an Axiovert

200 MOT microscope. Throughout, digital images were captured with a 40x/1.3 oil objective with the following filter sets:

- nanoparticles **1–SiO<sub>2</sub>**, and **2–SiO<sub>2</sub>**: Excitation 488 nm; Emission BP 500–530 for the donor part; Emission BP 565–615 for the acceptor part
- for ER-Tracker™ Blue-White DPX: Excitation 740 nm; Emission BP 435–485
- for Lysotracker® Green DND-26: Excitation 488 nm; Emission BP 500–530
- for nanoparticles **1a–SiO<sub>2</sub>**, and **2a–SiO<sub>2</sub>**: Excitation 543 nm; Emission BP 565–615

### Fluorescence microscopy for cassette **1–SiO<sub>2</sub>** nanoparticles (refers to Fig. 3a–b in article)

Clone 9 cells were incubated for 2 hours at 37 °C in serum free culture medium with 0.01 mg mL<sup>-1</sup> (10 µL) of doped nanoparticles (1 mg mL<sup>-1</sup> stock solution in PBS 7.4). After the incubation period, the cells were washed with serum free culture medium several times before imaging.

To confirm the subcellular localization of the nanoparticles, Clone 9 cells pre-treated with **1–SiO<sub>2</sub>** were co-incubated with 0.5 µm ER-Tracker™ Blue-White DPX (1 mM stock solution, Invitrogen®) in HBSS with Calcium and Magnesium for 30 min at 37 °C (ESI, Figure S4†).

### Fluorescence microscopy for **2–SiO<sub>2</sub>** nanoparticles (refers to Fig. 4a–b in article)

Clone 9 cells were incubated for 2 hours at 37 °C in serum free culture medium with 0.01 mg mL<sup>-1</sup> (10 µL) of doped nanoparticles (solution in PBS). After the incubation period, the cells were washed with serum free culture medium several times before imaging (ESI, Figure S5†).

## Acknowledgements

We thank The National Institutes of Health (GM72041), The Robert A. Welch Foundation (A1121) for financial support, the members of the TAMU/LBMS-Applications Laboratory for assistance with mass spectrometry.

## References

- 1 A. A. Burns, J. Vider, H. Ow, E. Herz, O. Penate-Medina, M. Baumgart, S. M. Larson, U. Wiesner and M. Bradbury, *Nano Lett.*, 2009, **9**, 442–448.
- 2 E. Herz, T. Marchincin, L. Connally, D. Bonner, A. Burns, S. Switalski and U. Wiesner, *J. Fluoresc.*, 2010, **20**, 67–72.
- 3 G.-S. Jiao, H. Thoresen Lars and K. Burgess, *J. Am. Chem. Soc.*, 2003, **125**, 14668–14669.
- 4 K. Burgess, *US Pat.*, US2005/0032120 A1, 2005.
- 5 K. Burgess, *US Pat.*, 2009/0192298 A1, 2009.
- 6 L. Wu, A. Loudet, R. Barhoumi, R. C. Burghardt and K. Burgess, *J. Am. Chem. Soc.*, 2009, **131**, 9156–9157.
- 7 J. Han, A. Loudet, R. Barhoumi, R. C. Burghardt and K. Burgess, *J. Am. Chem. Soc.*, 2009, **131**, 1642–1643.
- 8 J. Han and K. Burgess, *Chem. Rev.*, 2010, **110**, 2709–2728.
- 9 A. Burns, P. Sengupta, T. Zedayko, B. Baird and U. Wiesner, *Small*, 2006, **2**, 723–726.
- 10 J. Choi, A. A. Burns, R. M. Williams, Z. Zhou, A. Flesken-Nikitin, W. R. Zipfel, U. Wiesner and A. Y. Nikitin, *J. Biomed. Opt.*, 2007, **12**, 064007.

- 11 I. Miletto, A. Gilardino, P. Zamburlin, S. Dalmazzo, D. Lovisolo, G. Caputo, G. Viscardi and G. Martra, *Dyes Pigm.*, 2010, **84**, 121–127.
- 12 X. Xing, X. He, J. Peng, K. Wang and W. Tan, *J. Nanosci. Nanotechnol.*, 2005, **5**, 1688–1693.
- 13 Y.-S. Lin, C.-P. Tsai, H.-Y. Huang, C.-T. Kuo, Y. Hung, D.-M. Huang, Y.-C. Chen and C.-Y. Mou, *Chem. Mater.*, 2005, **17**, 4570–4573.
- 14 W. Sun, N. Fang, B. G. Trewyn, M. Tsunoda, I. I. Slowing, V. S. Y. Lin and E. S. Yeung, *Anal. Bioanal. Chem.*, 2008, **391**, 2119–2125.
- 15 I. I. Slowing, B. G. Trewyn and V. S. Y. Lin, *J. Am. Chem. Soc.*, 2007, **129**, 8845–8849.
- 16 I. I. Slowing, J. L. Vivero-Escoto, C.-W. Wu and V. S. Y. Lin, *Adv. Drug Delivery Rev.*, 2008, **60**, 1278–1288.
- 17 I. Slowing, B. G. Trewyn and V. S. Y. Lin, *J. Am. Chem. Soc.*, 2006, **128**, 14792–14793.
- 18 C.-Y. Lai, B. G. Trewyn, D. M. Jeftinija, K. Jeftinija, S. Xu, S. Jeftinija and V. S. Y. Lin, *J. Am. Chem. Soc.*, 2003, **125**, 4451–4459.
- 19 D.-M. Huang, Y. Hung, B.-S. Ko, S.-C. Hsu, W.-H. Chen, C.-L. Chien, C.-P. Tsai, C.-T. Kuo, J.-C. Kang, C.-S. Yang, C.-Y. Mou and Y.-C. Chen, *FASEB J.*, 2005, **19**, 2014–2016.
- 20 S. Giri, B. G. Trewyn, M. P. Stellmaker and V. S. Y. Lin, *Angew. Chem., Int. Ed.*, 2005, **44**, 5038–5044.
- 21 X. Huang, X. Teng, D. Chen, F. Tang and J. He, *Biomaterials*, 2010, **31**, 438–448.
- 22 J. M. Rosenholm, A. Meinander, E. Peuhu, R. Niemi, J. E. Eriksson, C. Sahlgren and M. Linden, *ACS Nano*, 2009, **3**, 197–206.
- 23 S. Kim, T. Y. Ohulchanskyy, A. Baev and P. N. Prasad, *J. Mater. Chem.*, 2009, **19**, 3181–3188.
- 24 R. Kumar, I. Roy, T. Y. Ohulchanskyy, L. N. Goswami, A. C. Bonoiu, E. J. Bergey, K. M. Tramposch, A. Maitra and P. N. Prasad, *ACS Nano*, 2008, **2**, 449–456.
- 25 J. Qian, X. Li, M. Wei, X. Gao, Z. Xu and S. He, *Opt. Express*, 2008, **16**, 19568–19578.
- 26 E. K. Stachowiak, I. Roy, Y.-W. Lee, M. Capacchietti, J. M. Aletta, P. N. Prasad and M. K. Stachowiak, *Integr. Biol.*, 2009, **1**, 394–403.
- 27 X. He, J. Duan, K. Wang, W. Tan, X. Lin and C. He, *J. Nanosci. Nanotechnol.*, 2004, **4**, 585–589.
- 28 D. J. Bharali, I. Klejbor, E. K. Stachowiak, P. Dutta, I. Roy, N. Kaur, E. J. Bergey, P. N. Prasad and M. K. Stachowiak, *Proc. Natl. Acad. Sci. U. S. A.*, 2005, **102**, 11539–11544.
- 29 J. E. Fuller, G. T. Zugates, L. S. Ferreira, H. S. Ow, N. N. Nguyen, U. B. Wiesner and R. S. Langer, *Biomaterials*, 2008, **29**, 1526–1532.
- 30 S. Kim, Y. Ohulchanskyy Tymish, E. Pudavar Haridas, K. Pandey Ravindra and N. Prasad Paras, *J. Am. Chem. Soc.*, 2007, **129**, 2669–2675.
- 31 T. Y. Ohulchanskyy, I. Roy, L. N. Goswami, Y. Chen, E. J. Bergey, R. K. Pandey, A. R. Oseroff and P. N. Prasad, *Nano Lett.*, 2007, **7**, 2835–2842.
- 32 C. Compagnin, L. Bau, M. Mognato, L. Celotti, G. Miotto, M. Arduini, F. Moret, C. Fede, F. Selvestrel, I. M. Rio Echevarria, F. Mancin and E. Reddi, *Nanotechnology*, 2009, **20**, 345101–345112.
- 33 H. Ow, D. R. Larson, M. Srivastava, B. A. Baird, W. W. Webb and U. Wiesner, *Nano Lett.*, 2005, **5**, 113–117.
- 34 A. Burns, H. Ow and U. Wiesner, *Chem. Soc. Rev.*, 2006, **35**, 1028–1042.
- 35 D. R. Larson, H. Ow, H. D. Vishwasrao, A. A. Heikal, U. Wiesner and W. W. Webb, *Chem. Mater.*, 2008, **20**, 2677–2684.
- 36 S. Santra, P. Zhang, K. Wang, R. Tapec and W. Tan, *Anal. Chem.*, 2001, **73**, 4988–4993.
- 37 D. Magde, R. Wong and P. G. Seybold, *Photochem. Photobiol.*, 2002, **75**, 327–334.
- 38 D. Magde, G. E. Rojas and P. G. Seybold, *Photochem. Photobiol.*, 1999, **70**, 737–744.
- 39 Y. Jin, S. Kannan, M. Wu and J. X. Zhao, *Chem. Res. Toxicol.*, 2007, **20**, 1126–1133.
- 40 A. S. Waggoner, *Methods Enzymol.*, 1979, **55**, 689–695.
- 41 W. J. Akers, M. Y. Berezin, H. Lee and S. Achilefu, *J. Biomed. Opt.*, 2008, **13**, 054042–054049.